9-27-2003

Predictability of seasonal runoff in the Mississippi River basin

Edwin P. Maurer
Santa Clara University, emaurer@scu.edu

Dennis P. Lettenmaier

Recommended Citation
Maurer, E.P. and D.P. Lettenmaier, 2003, Predictability of seasonal runoff in the Mississippi River basin, J. Geophys. Res. 108 (D16) 8607 doi:10.1029/2002JD002555

JOURNAL OF GEOPHYSICAL RESEARCH, VOL. 108, NO. D16, 8607, doi:10.1029/2002JD002555, 2003

Predictability of seasonal runoff in the Mississippi River basin

Edwin P. Maurer and Dennis P. Lettenmaier

Department of Civil and Environmental Engineering, University of Washington, Seattle, Washington, USA

Received 22 May 2002; revised 14 August 2002; accepted 15 August 2002; published 5 July 2003.

[1] Recent advances in climate prediction and remote sensing offer the potential to improve long-lead streamflow forecasts and to provide better land surface state estimates at the time of forecast. We characterize predictability of runoff at seasonal timescales in the Mississippi River basin due to climatic persistence (represented by El Niño-Southern Oscillation and the Arctic Oscillation) and persistence related to the initial land surface state (soil moisture and snow). These climate and land surface state indicators, at varying lead times, are then used in a multiple linear regression to explain the variance of seasonal average runoff. Soil moisture dominates runoff predictability for lead times of 1 1/2 months, except in summer in the western part of the basin, where snow dominates. For the western part of the basin, the land surface state has a stronger predictive capability than climate indicators through leads of two seasons; climate indicators are more important in the east at lead times of one season or greater. Modest winter runoff predictability exists at a lead time of 3 seasons due to both climate and soil moisture, but this is in areas producing little runoff and is therefore of lessened importance. Local summer runoff predictability is limited to the western mountainous areas (generating high runoff) through a lead of 2 seasons. This could be useful to water managers in the western portion of the Mississippi River basin, because it suggests the potential to provide skillful forecast information earlier in the water year than currently used in operational forecasts. *INDEX TERMS:* 1833 Hydrology: Hydroclimatology; 1860 Hydrology: Runoff and streamflow; 1863 Hydrology: Snow and ice (1827); 1866 Hydrology: Soil moisture; *KEYWORDS:* hydroclimatology, predictability, soil moisture, Mississippi River basin, runoff

Citation: Maurer, E. P., and D. P. Lettenmaier, Predictability of seasonal runoff in the Mississippi River basin, *J. Geophys. Res.*, *108*(D16), 8607, doi:10.1029/2002JD002555, 2003.

1. Introduction

[2] The history of the United States, and especially its expansion westward, is inextricably tied to water. Beginning with the Homestead Act of 1862, the federal government actively promoted settlement of the arid and semi-arid west. Incentives were increased as the available lands became less fertile and more arid. The Reclamation Act of 1902 was transformed in the early 1930s into a major land and water development program, and the period of settlement that ended around 1900 was followed by a period of intense construction of increasingly large, multipurpose water projects, which continued into the 1960s. As the better dam sites were developed and their economic feasibility came into question, and with a mounting environmental opposition, the emphasis in water policy shifted toward management of resources [e.g., *Plummer*, 1994; *Beard*, 1994; *Marston*, 1987]. This last period, which continues today, arguably began with the Wild and Scenic Rivers Act of 1968. With population of the United States projected to rise by 20 percent by 2020 [*U.S. Census Bureau*, 2000] and the West, where water scarcity is greatest, by up to 30 percent [*Western Water Policy Review Advisory Commission*, 1998], water planners are being forced to look for new opportunities for better management of a resource that is now essentially fully developed. In addition, some have argued that climate change may increase water scarcity in areas of the United States where water supplies generally are not currently constrained [*Intergovernmental Panel on Climate Change*, 2001, chap. 4; *National Assessment Synthesis Team*, 2001; *Vörösmarty et al.*, 2000].

[3] Aside from structural changes in water use (e.g., reallocation of water, such as from agriculture to municipal and industrial), perhaps the greatest potential for improving water management is through more accurate streamflow forecasting. Over the last decade, great strides have been made in two areas that offer considerable potential for improved streamflow forecasting. The first is better understanding of climate teleconnections as manifested by ocean-atmosphere phenomena such as El Niño-Southern Oscillation (ENSO), the Pacific Decadal Oscillation, and the Arctic Oscillation (AO). A second opportunity is use of remote sensing products for better initialization of the hydrologic system [e.g., *Walker and Houser*, 2001; *Pauwels et al.*, 2001; *Rango et al.*, 2000; *Carroll et al.*, 1999]. These include snow cover extent, snow water equivalent, and surface skin temperature. All of these variables are observed, with various limitations, by existing sensors, the resolution and quality of which have improved with launch

0148-0227/03/2002JD002555

of Earth Observing System (EOS) Terra and Aqua platforms, and with planned soil moisture missions [*Hall et al.*, 2002; *Ma et al.*, 2002; *Njoku and Li*, 1999; *Kerr et al.*, 2001].

[4] Improved knowledge of climate dynamics has resulted in demonstrable improvements in long-lead (to lead times as long as a year) climate forecasts, based on coupled ocean-atmosphere-land models [e.g., *Goddard et al.*, 2001, and references therein]. Teleconnections of climate signals, especially ENSO and also the AO, have been established for the United States for precipitation and temperature [*Higgins et al.*, 2000; *Livezey and Smith*, 1999; *Kumar and Hoerling*, 1998; *Gershunov*, 1998; *Wang et al.*, 1999], snowfall [*Kunkel and Angel*, 1999], and streamflow [*Dracup and Kahya*, 1994; *Kahya and Dracup*, 1993]. Despite the presence of apparent predictability in the climate signal, and the teleconnections to land surface hydrologic variables, the incorporation of climate forecasts in forecasts of seasonal runoff (or streamflow) has thus far been largely limited to experimental settings [e.g., *Wood et al.*, 2002; *Baldwin*, 2001; *Garen*, 1998; *National Water and Climate Center*, 1998]. Monthly to seasonal streamflow forecasts widely used in the western United States more commonly rely on regression-based forecasts [*Soil Conservation Service*, 1988; *Garen*, 1992], or use hydrologic simulation models to capture the hydrologic memory, as reflected in soil moisture and snow storage, and then assume, explicitly or implicitly, climatological average conditions during the forecast period [e.g., *Twedt et al.*, 1977]. We contend that recent advances in climate prediction and remote sensing provide the capability to improve long-lead streamflow forecasts by utilizing climate forecasts, and by incorporating better estimates of the state of the land surface at the time of forecast, a contention that we evaluate for the domain of the Mississippi River basin in the remainder of this paper.

[5] *Hornberger et al.* [2001], in their assessment of global water cycle research necessary to address critical water problems facing society, identified as one of their three key science questions the predictability of variations in the global and regional water cycle. The *National Research Council* [2002] built on that assessment and raised the questions of whether accurate observation of initial land surface conditions increases hydrometeorological predictability, and when and where this predictability is likely to be most important. In this study, we address these questions by taking advantage of a recently developed hydrologically based land surface data set [*Maurer et al.*, 2002] to characterize hydrological predictability due to climatic persistence and persistence related to the initial state of the land surface. We focus on distributed runoff (e.g., spatial fields of runoff) rather than the space-time convolution of runoff (streamflow), in order to identify regional patterns and influences in runoff predictability. The primary questions we address are as follows: (1) During which seasons is the predictability of runoff greatest? (2) How does the contribution of initial hydrologic conditions relative to climate predictability vary geographically? (3) Where are potential improvements in seasonal runoff forecast accuracy due to improved observations (e.g., through remote sensing or in situ observations) of the land surface moisture state the greatest? We focus our attention on the Mississippi River basin (Figure 1), which coincides with the study area of the World Climate Research Programme's Global Energy and Water Cycle Experiment (GEWEX) Continental-Scale International Project (GCIP), a project established with the long term goal of demonstrating skill in predicting changes in water resources on timescales up to seasonal, annual and interannual [*World Meteorological Organization*, 1992].

2. Methods and Data

[6] The gridded data set of land surface and climatic variables of *Maurer et al.* [2002] is used to determine the predictability of runoff throughout the Mississippi River basin from currently available, or potentially available information. Details of the data derivation and validation are given by *Maurer et al.* [2002]. To summarize briefly, the runoff data were produced using the Variable Infiltration Capacity (VIC) hydrologic model driven by observed precipitation and temperature, and other derived surface radiative and meteorological forcings (see *Liang et al.* [1994] and *Cherkauer et al.* [2003] for details of the model structure). The model was run at a 3-hour time step for the period January 1950 to July 2000, with a grid cell size of 1/8 degree (approximately 140 km^2 per grid cell). Throughout this paper, predictability is assessed for seasonal average runoff on a grid cell by grid cell basis for a range of lead times for hydrologic and climatic initial conditions extracted from the *Maurer et al.* [2002] data set, as shown in Figure 2. Following the convention of *Barnston* [1994], the lead time is the number of seasons "skipped" between the predictor(s) and the predictand, so a lead-0 indicates a lead time of 1.5 months from the initialization to the midpoint of the predicted season. Seasons are defined as December–February (DJF), March–May (MAM), June–August (JJA), and September–November (SON). The date on which initial conditions are determined, i.e., the initialization date or date of forecast, is shown with vertical lines in Figure 2 for the example of predicting DJF runoff. Because we use climate and land surface variables on the initialization date to predict runoff in a future season, we do not include any runoff forecast skill obtainable through predictability of the evolution of these variables. For the case of climate initial conditions, this is discussed in more detail in section 2.2.

[7] Climate indicators (represented in this study by the Southern Oscillation Index, SOI, and the Arctic Oscillation, AO, Index: see section 2.2) and land surface state (snow water equivalent, SWE, and soil moisture, SM: see sections 2.3 and 2.4, respectively) influence seasonal runoff as indicated in Figure 3, which shows schematically the effect of unpredictable weather noise in the climate system. Note that we ignore the possibility of an additional noise component between the soil moisture and snow states and runoff in this study. Because the runoff and land surface states in the *Maurer et al.* [2002] data set are derived from the same model simulation, the only direct effect of noise on runoff in the data set is though the unpredictable weather component that drives the hydrologic model.

[8] For this study, we consider only the initial conditions of the climate indicators and land surface moisture state as predictors of future runoff, so the process illustrated in Figure 3 is "one-way," in that no feedback from the initial land surface moisture state to climate evolution is included.

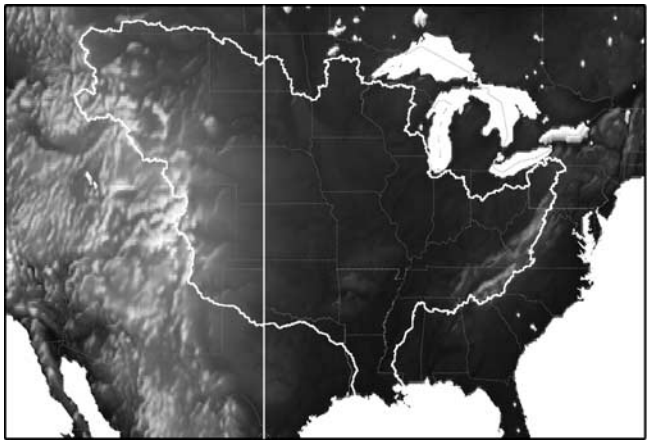

Figure 1. Location of the Mississippi River basin in North America. The basin boundary is shown in white, as is a north-south line at longitude 100°W.

Initial soil moisture, varying between extreme wet and dry initial states, has been shown to greatly change 30-day forecasts of precipitation averaged over regional to continental areas [*Beljaars et al.*, 1996; *Betts et al.*, 1996], though the effects of initial soil moisture anomalies representative of typical interannual variability have been shown to have little impact on the evolving atmosphere [*Oglesby et al.*, 2002]. Because we include initial soil moisture explicitly as a predictor, any predictability due to feedback to the atmosphere, at least that which can be captured by the linear relationships used in this study, is attributed to knowledge of the initial moisture state rather than knowledge of climate evolution due to initial land surface state.

2.1. Evaluation of Predictability

[9] To assess the predictability of seasonal average runoff, we used multiple linear regression, using as predictors various combinations of the SOI, AO, SM, and SWE at different lead times. The regressions were performed on a grid cell by grid cell basis across the domain. The multiple regression equations developed for the combinations of variables are not used as predictive models; only the variance explained by the regression is used. The values of the variance explained by the predictors, r^2 (where r is the correlation coefficient of the regression) were plotted spatially at the different lead times to illustrate their predictive capability of seasonal runoff by season and by lead time. The predictor variables are assigned to three tiers, where the climate indicators that are currently available for incorporation into forecasts, are assumed to be the best known variables, and SWE, which in practice is estimated by ground surveys and remote sensing, is less known, and SM is essentially unobserved, and hence is least well known. The variances explained by each tier are the incremental amounts over and above that already explained by better known variables. In this way, variances explained by two correlated variables are only counted once, and are attributed to the better known variable.

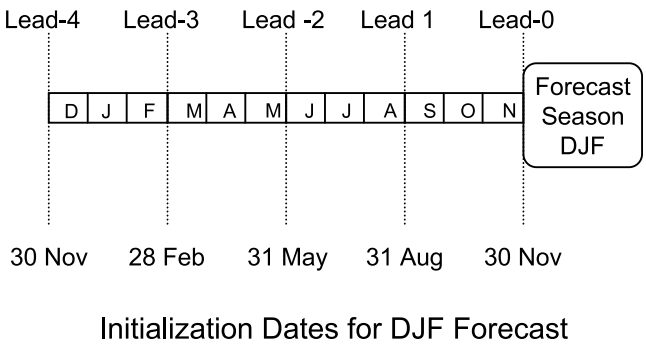

Figure 2. Example of initialization dates for forecasting the DJF runoff at lead times of 0 through 4 seasons.

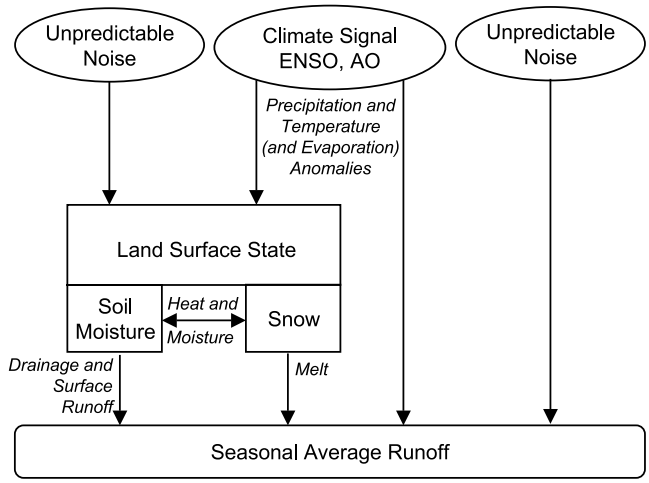

Figure 3. Schematic of the predictable and unpredictable influences on seasonal runoff considered in this study. Note that for this study the interactions are one-way; feedback from the land surface to climate is not considered: Only the initial conditions of the climate indicators are included.

[10] To test for significant correlations, the two-step process outlined by *Livezey and Chen* [1983] was used. First, temporal autocorrelation was taken into account, and the effective number of temporal degrees of freedom was determined. As applied in this study, the time between independent samples was computed for each grid cell for each combination of predictors as [*Livezey and Chen*, 1983]

$$\tau_P = \left[1 + 2\sum_{i=1}^{N} C_P(i\Delta t)C_R(i\Delta t)\right]\Delta t \qquad (1)$$

where C_P is the autocorrelation function for the selected combination of predictors (separated by season, e.g., a 50 year sequence of DJF values of SOI), C_R is the autocorrelation function of the seasonal runoff, i is the sample number of N total samples, and Δt is the sampling time (one season for this study), so $i\Delta t$ represents a lag of i seasons. The effective number of degrees of freedom, n, was then determined by [*Livezey and Chen*, 1983]

$$n = \frac{N\Delta t}{\tau_P} \qquad (2)$$

At each grid cell the computed value of the correlation coefficient r was compared against the 95% significance

Table 1. Fractional Area Thresholds (Expressed as Percentages of Entire Mississippi River Basin Area Exhibiting Local Significance) That Must be Exceeded to Achieve Statistical Field Significance at a 95% Confidence Level

	Lead (DJF)					Lead (MAM)					Lead (JJA)					Lead (SON)				
Predictors	0	1	2	3	4	0	1	2	3	4	0	1	2	3	4	0	1	2	3	4
ALL	54	42	44	54	58	53	52	40	43	53	40	50	51	40	40	41	41	53	54	40
SOI AO	29	28	27	28	27	24	24	26	25	26	25	29	28	27	28	27	24	24	26	25
SWE	10	8	8	10	10	9	9	8	8	9	8	10	11	8	9	8	8	9	10	8
SM	10	8	8	9	9	9	8	8	8	9	8	10	8	8	9	9	9	8	8	8

criterion for no correlation, which provided a determination of local significance.

[11] The total amount of significant area was determined by counting the number of grid cells exhibiting locally significant correlation, with each grid cell weighted by the cosine of latitude to avoid biasing due to differences in grid cell area. If there were no spatial correlation and each grid cell (there are 1532 1/2-degree grid cells in the Mississippi River basin) were an independent sample, we would expect 5% of the grid cells (77) to show significant correlation by chance 6% of the time, based on the binomial distribution. At lead times and seasons where greater than 6% of the area showed local significance, statistical field significance at the 95% confidence level would be claimed. Because there is spatial correlation between grid cells in the runoff fields (as well as in SM and snowfields), the actual number of spatial degrees of freedom is considerably less than 1532. As a first estimate, the number of empirical orthogonal functions needed to describe 95 percent of the variance in seasonal runoff varies from 35 in DJF to 39 in JJA, which translates to 15.2–15.8% of the area that would show local significance by chance. As a practical matter, this suggests a need to use a Monte Carlo technique to assess spatial field significance.

[12] Monte Carlo simulations were performed in a manner similar to that of *Barnston* [1994], in which the forecast to observation year correspondence was randomly shuffled over the entire domain, and the fractional area of the basin exhibiting significant correlation at a 95% level based on a t-test was computed. The process was repeated 500 times for each lead time, season, and set of predictors. For each season and lead time the area determined as significant by this Monte Carlo technique is the minimum for a result to achieve statistical field significance. Table 1 shows the results of these Monte Carlo simulations, and the minimum area with significant correlations for field significance. It should be noted that field significance is a basin-wide test in this study. If a particular (a priori) interest were exclusively in one sub-area of the basin, then local significance would still be pertinent, though basin-wide field significance of this may not. A separate set of Monte Carlo experiments for only the area of interest could be used to determine the area required for field significance of a sub-area.

2.2. Climate Signals

[13] Given the established teleconnections of climate signals with hydrologic variables over the United States (see references in section 1), our objective was to characterize the seasonal predictability of runoff, and the dominant sources of predictability. At seasonal to interannual scales, the El Niño-Southern Oscillation (ENSO) is the best known and most prominent predictable climate signal [*Rasmussen and Wallace*, 1983]. One index used to quantify the phase of the ENSO signal is the SOI, which is based on the surface pressure difference across the South Pacific (Tahiti minus Darwin). The SOI has been related to various land surface effects in the continental United States, including seasonal temperatures [*Wolter et al.*, 1999], precipitation [*McCabe and Dettinger*, 1999], and streamflow [*Cayan et al.*, 1999]. Because of this past use of the SOI in teleconnection studies we decided to use it in this study as well, and we obtained the monthly standardized difference index from the National Oceanic and Atmospheric Administration, National Centers for Environmental Prediction Climate Prediction Center (http://www.cpc.ncep.noaa.gov/data/indices/). *Trenberth* [1997] recommends smoothing of the monthly SOI index to remove the effect of high-frequency, small-scale phenomena. As given by *Ropelewski and Jones* [1987], we applied a five-month moving average to the monthly SOI time series. Although the effect of this smoothing is to include some future information of SOI state in the value for the current month, we argue that that the smoothing, by removing high-frequency fluctuations, makes the SOI more comparable to the more slowly varying sea surface temperature (SST)-based ENSO indicators. For example, the unsmoothed SOI has a correlation with the SST index Niño 3.4, for the period 1950–1999 of −0.72, while 5-month smoothing of SOI produces a stronger correlation of −0.87. The smoothing therefore results in SOI values that more closely resemble the SST-based index that would be available at the time of forecast. These values can be used as an indicator of climate state that would be known at the initialization time, with the results of the predictability analysis being more robust, irrespective of the ENSO index chosen.

[14] *Shukla* [1998] suggested that the evolution of ENSO events appears to be predictable 6 to 9 months in advance, and that SOI-based persistence forecasts may underestimate the predictability of sea surface temperature anomalies. *Barnston et al.* [1999] subsequently showed that both coupled GCMs and statistical models outperform simple persistence in forecasts of ENSO state at lead times of 3.5 to 9.5 months. *Landsea and Knaff* [2000] argued that a more reasonable baseline of ENSO predictability than simple persistence is a simple statistical model such as the ENSO climatology and persistence (ENSO-CLIPER) model [*Knaff and Landsea*, 1997]. *Landsea and Knaff* [2000] show that this simple regression-based model outperformed coupled GCMs and more complex statistical models for predicting the 1997–1998 El Niño event for lead times through two seasons, though for 3 and 4 season forecast lead times a modest improvement was achieved using a more sophisticated statistical model. The factors influencing the characteristics of an El Niño event, and ultimately its predictability, differ for each event [*Philander*, 1999; *Fedorov*, 2002]. This implies that the predictability of an El Niño event achieved

by any particular model will vary with each event, hence the relative skill attributed to coupled GCMs, statistical or persistence forecasts will change accordingly. Although the ENSO-CLIPER model will not outperform GCM forecasts for all historical El Niño events, we use the ENSO-CLIPER model to generate forecasts of SOI to estimate of the potential difference in runoff predictability between simple persistence and forecasted ENSO state.

[15] *Barnston et al.* [1999] note that success in forecasting sea surface temperatures does not necessarily imply comparable success in forecasting impacts in teleconnected regions such as the continental United States The process of translating a predicted sea surface temperature anomaly into a remote land surface response introduces additional unpredictable noise, so that a marginal increase in prediction of ENSO will not necessarily result in measurable increase in predictability of the land surface effects associated with ENSO. In particular, the selection of an ENSO indicator used in persistence mode, or with a model to predict its evolution, may not result in substantially different land surface predictability.

[16] To test whether, for predictions of seasonal runoff, there is any change in apparent potential skill between using the simple persistence of initial SOI relative to SOI forecasted by a statistical model, the ENSO-CLIPER model was obtained (from http://www.aoml.noaa.gov/hrd/Landsea/ensocliper/). It was run from 1951 (the earliest year for which required input data are available) through July 2000, with the climatological SOI values added for 1950 to make the record consistent with the period of record for the land surface variables included in this study. The SOI used for testing the simple persistence model was the smoothed SOI index discussed above.

[17] Seasonal average runoff values at each grid cell were regressed against the smoothed SOI values in a persistence mode: that is, against the SOI value for the appropriate initialization date for each season and lead times of 0, 1, and 2 seasons. Spatial plots of the variance explained by this SOI initialization (persistence mode) are shown in Figure 4a. For comparison, the seasonal runoff at each grid cell was also regressed against the ENSO-CLIPER forecasted SOI values. First, the ENSO-CLIPER model was initialized on the appropriate initialization date, after which seasonal average values of SOI were forecasted for each lead time. These forecasted SOI values were regressed against the seasonal average runoff for the same season. The runoff variance explained using ENSO-CLIPER forecasted SOI values is plotted in Figure 4b. The patterns exhibited in these two figures are in general very similar. This suggests that, although ENSO-CLIPER shows better sea surface temperature forecast skill (as measured by root mean square error, RMSE) than simple persistence (at least for the event studied by *Landsea and Knaff* [2000]), consistent with the discussion above, the marginal increase of ENSO predictability does not translate to a measurable increase in land surface predictability. We conclude that the use of the SOI forecasts produced by the ENSO-CLIPER model has a negligible effect on the skill of seasonal runoff predictability in the Mississippi River basin as compared to using SOI values in a persistence mode. Furthermore, because the RMSE of ENSO-CLIPER is shown by *Landsea and Knaff* [2000] to be 49–66% lower than the simple persistence

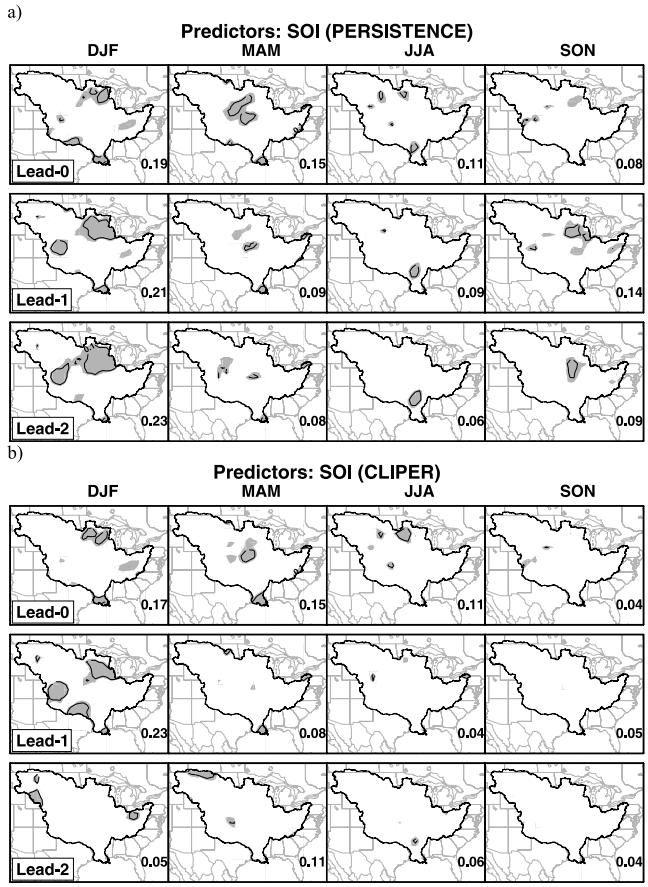

Figure 4. Predictability of seasonal runoff due to SOI, expressed as the fractional variance, r^2, of seasonal runoff explained by SOI, using (a) a simple persistence model and (b) the ENSO-CLIPER model. Countour intervals of r^2 values are every 0.1, and shading indicates locations where the r^2 is statistically significant. In the lower right corner of each panel is the fraction of the total basin area with significant correlation.

model for leads of 0–2 seasons, with no measurable benefit for runoff forecasting, the additional improvement (reflected by a further RMSE reduction by 18–24%) of more sophisticated statistical models compared to ENSO-CLIPER at leads of 3–4 seasons would not be expected to provide additional predictability of seasonal runoff over the persistence model. We conclude therefore that for our purposes, treating SOI in a persistence manner (that is, discarding knowledge of the climatological evolution of ENSO events), produces results that are comparable to those achieved by using a more sophisticated statistical model.

[18] Recent studies show that additional predictability of air temperature and precipitation, particularly in winter, can be obtained over portions of the United States by incorporating the modes of the AO, which encompasses the North Atlantic Oscillation [e.g., *Higgins et al.*, 2000; *Rohli et al.*, 1999; *Lin and Derome*, 1998]. Operational seasonal climate predictions for the United States currently are capable of exploiting strong ENSO signals to improve forecast skill. It has been argued [*Baldwin and Dunkerton*, 2001; *Higgins et al.*, 2000] that future forecast improvements will require the

ability to predict subtler changes in ENSO conditions, as well as the AO. For this reason, we use two indices to represent the predictability of seasonal runoff due to climate signals: the 5-month smoothed SOI index and the AO. Values of SOI for the initialization day were interpolated by averaging the two adjacent monthly values of the filtered SOI. To characterize the mode of the AO, an AO index was obtained (from http://www.atmos.colostate.edu/ao/Data/ao_index.html; see *Thompson and Wallace* [1998, 2000] for details). The AO index for the initialization day (date of forecast) was interpolated from adjacent monthly values, as for the SOI.

2.3. Snow

[19] In areas where a substantial fraction of precipitation falls as snow, water stored in the snowpack can be released months later, providing a source of persistence that can be exploited in seasonal streamflow forecasting. In the United States, seasonal streamflow forecasts have been based on estimates of the amount of water stored in the snowpack since at least 1900 [*Church*, 1937]. Individual snow surveys (which, in automated form, remain at the heart of the streamflow forecasts produced by the National Resources Conservation Service [*Soil Conservation Service*, 1988]) are (or were, prior to automated data collection) time consuming and cover relatively small areas. The need for a better spatial context for estimates of the snow state inspired early attempts to use panoramic photographs for forecasting runoff from snowmelt [*Potts*, 1937]. Because photographs provide a basis for estimating snow covered area (SCA) rather than the water equivalent of the snowpack, approaches based on SCA necessitated the development of methods to deduce snow water content from spatial coverage. In the satellite era, remotely sensed products have provided estimates of SCA, which have shown to have value for runoff forecasting [e.g., *Rango and Martinec*, 1979]. Although methods have been developed for direct estimation of the water content of the snowpack (or SWE) via remote sensing [e.g., *Goodison and Walker*, 1995; *Shi and Dozier*, 2000], and new sensors such as the Advanced Microwave Scanning Radiometer (launched in May 2002 on NASA's Aqua platform) hold promise for future SWE measurements, these methods have not been available operationally [*Rango et al.*, 2000] and cannot provide the length of record needed for this study of the variability of SWE in the context of runoff predictability.

[20] Therefore, for assessing potential predictability due to knowledge of initial snow water storage, we use the derived snow water equivalent product in the *Maurer et al.* [2002] data set. The snow water equivalent used for prediction is the value for the last (3-hour) time step of the last day of the month prior to the beginning of the forecast season. We believe that this is a reasonable surrogate for the initial snow water equivalent condition that would be available at the forecast time, and therefore represents the maximum level of predictability obtainable through error-free observations of the water equivalent of the snowpack.

[21] In order to avoid spurious correlations due to poorly conditioned probability distributions of SWE in areas that usually are snow-free, we apply a threshold to the SWE data at each grid cell. During the entire period of 51 years, we require for each season that during at least 10 of the years a minimum of 0.1 mm of SWE must be on the ground in order for SWE to be included as a candidate predictor.

2.4. Soil Moisture

[22] In addition to the water stored as snow, the water stored in the soil column exhibits seasonal and interannual persistence that can be exploited in seasonal forecasts. It has been well known from the early days of hydrologic prediction that SM plays a key role in predicting the effect of a given precipitation pattern on the resulting runoff response of a watershed [e.g., *Linsley and Ackerman*, 1942]. Despite its importance to hydrologic modeling and runoff forecasting, SM lacks a good observational database [*Dirmeyer*, 1995].

[23] Given the expense and difficulty of collecting SM measurements, alternative techniques are being implemented that offer promise for better determination of SM state, and hence better definition of initial conditions for forecasting seasonal water supply. Two recent advances that offer the potential to provide more accurate estimates of SM conditions for runoff prediction are macroscale hydrologic modeling and remote sensing. The North American Land Data Assimilation (LDAS) experiment (K. Mitchell et al., The GCIP Land Data Assimilation (LDAS) Project: Now underway, *GEWEX News*, *9*(4), 3–6, 1999) simulates SM fields in real-time over the continental United States using observations of precipitation and temperature to drive a suite of several land surface models. Shortcomings of SM estimates produced using this technique include errors in forcing data due to the inhomogeneity and low station density of near-real-time meteorological observing stations [*Groisman and Legates*, 1994], and the effects of model and parameter errors on the generated SM fields [*Schaake et al.*, 2002].

[24] The most promising method for estimating soil moisture via remote sensing is based on remote sensing using passive microwave instruments operating at long (in excess of 10 cm) wavelengths. A key technological constraint that has precluded spaceborne remote sensing of soil moisture to date is the tradeoff between the need for long wavelengths to penetrate soil to sufficient depths (which in any event are limited to a few cm) and to avoid obscuring the signal with vegetation water, and the requirement for large antennas to achieve adequate spatial resolution consistent with hydrological and atmospheric models (e.g., 10–25 km) at long wavelengths. The advanced scanning microwave radiometer (AMSR) instrument on board the EOS Aqua platform (launched 4 May 2002) has a 4.3 cm wavelength for one of its channels, which although not ideal for soil moisture sensing, provides some capabilities in regions of sparse vegetation cover. The current observations of SM, sparser and less consistent than observations of SWE, do not cover a time period or have a spatial resolution adequate for the investigation in this study.

[25] Therefore, for this study, we used an index of SM, specifically the total moisture in the soil column on the forecast initialization date from the derived data set of *Maurer et al.* [2002]. Notwithstanding the inability at present to observe SM directly, the *Maurer et al.* [2002] data set can be considered to be a surrogate for the best information that may eventually be available through a combination of remote sensing and modeling. As such, it can be considered to provide an upper limit on the infor-

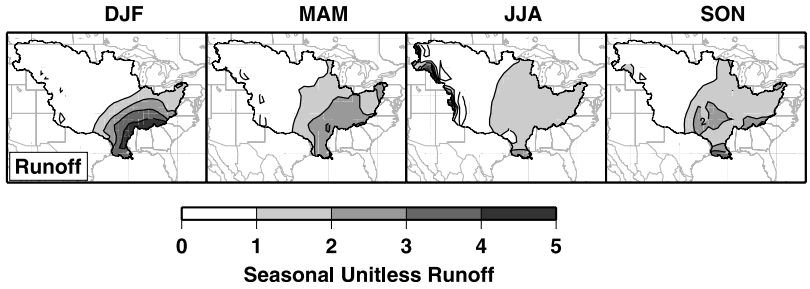

Figure 5. Average seasonal runoff for the Mississippi River basin, divided by the seasonal basin-wide average.

mation content that would be available from high-quality observations, and its use is consistent with our attempts to estimate potential runoff predictability.

2.5. Runoff Data

[26] The runoff data used in this study were the derived product archived by *Maurer et al.* [2002]. For this study we aggregated the 3-hourly runoff values to monthly and seasonal averages. Furthermore, we aggregated spatially from the 1/8 degree native spatial resolution of the data set to 1/2 degree spatial resolution, in order to reduce array sizes and produce a more computationally tractable data set. As shown by *Maurer et al.* [2002] the runoff, when routed through a channel network to basin outlet points, closely matches observed streamflows throughout the basin.

3. Results and Discussion

3.1. Seasonal Runoff Magnitude

[27] The magnitude of runoff in the Mississippi River basin varies considerably across the domain and throughout the year. Figure 5 shows the seasonal runoff, expressed as the average runoff at each grid cell divided by the basin-wide average runoff for each season. For example, most of the DJF runoff is produced in the southeastern part of the basin, and the highest JJA runoff is produced along the western edge of the basin, in the Rocky Mountains. Seasonal predictability is generally of greatest value where (a) runoff volumes are high, as it indicates potential for forecast skill that could affect a relatively large part of the annual runoff, and/or (b) in locations where infrastructure (such as large reservoirs) exists to allow water managers to respond to long lead forecast information.

3.2. Total Runoff Predictability

[28] Figure 6 shows the total variance of seasonal runoff explained by the climatic and land surface predictors together. The shading highlights areas with locally statistically significant correlation. Shown on each plot are the fractions of the basin with significant local correlation, which were compared with the threshold values in Table 1 to test for field significance. Statistical field significance exists in DJF for leads up to and including 3 seasons, while MAM and SON runoff predictability shows field significance at leads through one season. The JJA season shows field significance through a lead of 1 season and also at a lead of 4 seasons.

[29] For DJF runoff predictability, a very large percentage (up to 70%) of the runoff variance at lead-0 is explained in the northern and western areas of the basin, while Figure 5 shows the greatest runoff occurs in the south and east. These very high levels of predictability in the western mountains are due to three combined effects: (1) precipitation is low during this season and snowmelt is limited, so direct surface runoff is low; (2) the runoff leaving each grid cell is drained from the lower soil layers; and (3) in the VIC model used to produce the data given by *Maurer et al.* [2002], the rate of soil moisture drainage is controlled by the moisture level in the lowest soil layer. During MAM at lead-0, the variance explained by the predictors drops to 30–50% through most of the northern and western portions of the basin, with the lowest values tending to occur where runoff is highest. The

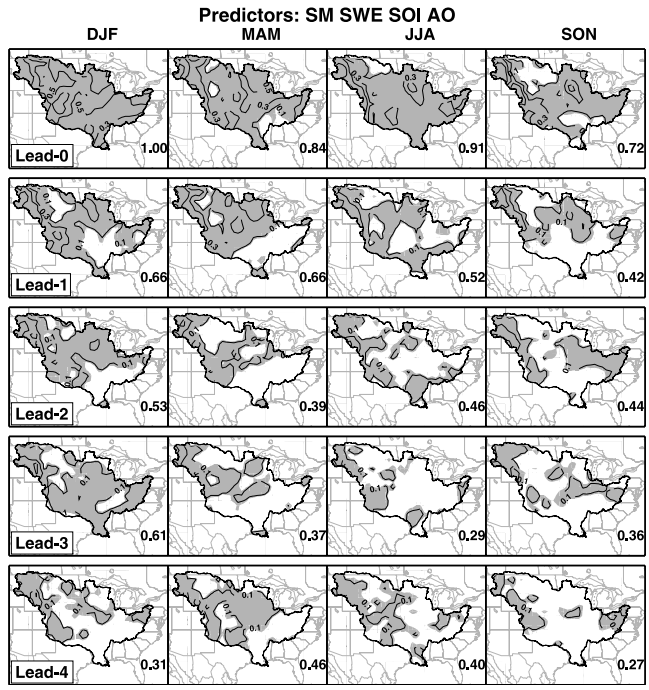

Figure 6. Predictability of seasonal runoff for each season (columns) and each lead time (rows), using combined climatic and land surface predictors, SOI, AO, SM, and SWE. Predictability is defined as the fractional runoff variance explained by the predictors, r^2, in a multiple linear regression. Contour interval is 0.1, with locally significant r^2 values shaded. The number in the lower right corner of each panel indicates the fraction of the basin exhibiting local statistical significance; this number is used in comparison with the field significance thresholds in Table 1.

JJA runoff variance explained by the predictors is more uniform throughout the basin, with a concentration of higher values along the mountainous western extreme of the basin, which coincides with the highest runoff values in Figure 5. JJA runoff predictability in this region is of particular importance, because it provides the water supply used to fill large reservoirs throughout the western part of the basin. It is this predictability that is exploited by streamflow forecasters in the west to anticipate available water supply. Typically this forecasting of MAM and JJA runoff begins in January. This figure shows that, using climatic indicators and knowledge of the land surface moisture state some measure of locally significant runoff predictability exists for the mountainous western area of the basin for lead times of 4 seasons, which would be a valuable extension of the current forecasts. By partitioning this predictability we will examine the sources of this total predictability during different seasons and at different lead times.

3.3. Runoff Predictability Due to Climate

[30] Figure 7 shows the runoff variance explained by the climatic predictors. Because these predictors (SOI and AO indices) are both available in near real-time, this represents a source of runoff predictability that is realistically achievable (discounting the effect of the 5-month smoothing of SOI). Applying the threshold values from Table 1, statistical field significance can be claimed for DJF at a lead of 0 seasons, and also at leads of 2 and 3 seasons. Runoff in MAM and JJA shows field significance through a 0 season lead, and SON shows no field significance for any leads. This is consistent with the observation that ENSO [e.g., *Kumar and Hoerling*, 1998] and AO [e.g., *Higgins et al.*, 2000] signals typically exhibit their strongest signals in boreal winter. Although the runoff variance explained for DJF at a lead of three seasons is generally low (about 10%) its field significance and its overlap, at least partially, with areas of high runoff (Figure 5) suggest that these climate indicators may be capable of providing valuable predictive information for runoff in the Mississippi River basin at leads of greater than 9 months. For the mountainous extreme western portion of the basin, even with relatively small areas showing significant amounts of JJA runoff variance explained at leads of two and three seasons, the relatively high runoff produced by these areas (Figure 5) during JJA implies a potential local benefit for including climatic indicators at these leads, despite the lack of field significance at a basin-wide level.

[31] For DJF runoff, the coincidence of areas with high runoff with modest, but statistically significant, runoff predictability at long indicates that for prediction of DJF runoff, climatic indicators may be the most important source of long-lead predictability. This also illustrates a complication in using persistence of climate signals for prediction, as is done in this study. Specifically, noting the significant runoff predictability in the southeastern (Gulf) region of the basin at a lead of 3 seasons, this predictability vanishes at shorter leads of 1 and 2 seasons. *Dracup and Kahya* [1994] discuss one potential explanation for this phenomenon (in their case, it apparently occurs because observations of the La Niña phase of the ENSO cycle during winter and spring in the Gulf region of the United States are typically followed by anomalously wet conditions the next year). Although the results shown in Figure 7 include the effects of both ENSO and AO, this highlights the point that the predictability due to climate is not necessarily due to persistence of the climate signals, but may reflect a regionally specific response to climatic forcing. It should also be stressed that this analysis is based on a 50 year record, and individual events in each season may have differing sources and levels of predictability that do not match this general climatological predictability indicator.

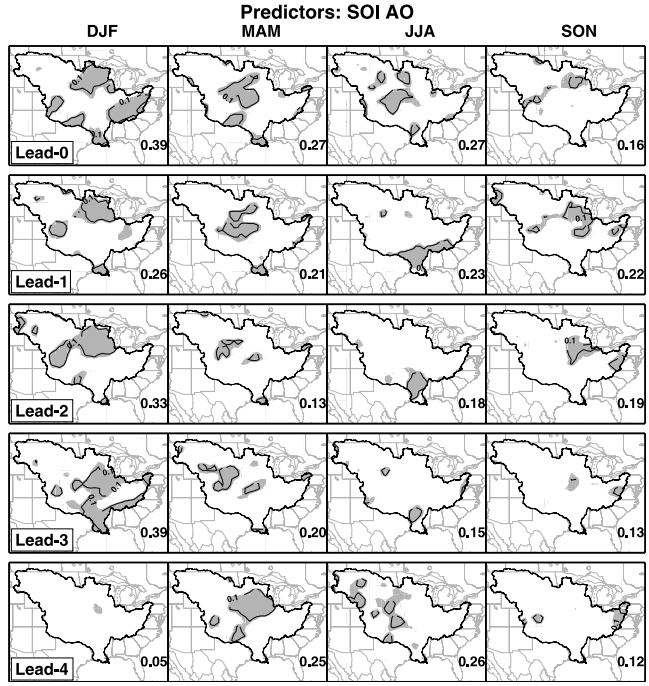

Figure 7. Same as for Figure 6, but including only climatic indicators, SOI and AO as predictors.

3.4. Runoff Predictability Due to Snow State

[32] The climatic indicators we use as predictors are based on direct and readily available observations, whereas the soil and snow moisture states are based on perfect knowledge of the land surface moisture state. Because both SM and SWE are driven by the same climatic factors, and by their nature interact with one another, they can be highly correlated. Figure 8 shows the correlation coefficient between SWE and SM for each season. Not surprisingly, the two tend to be correlated most strongly in areas undergoing episodes of snowmelt, thus MAM shows high correlations over the northern and western areas, while the mountainous areas along the extreme west show very high correlation in JJA.

[33] Because of the longer history of remote sensing of snow and the wider array of ground observations as compared to SM, for comparative purposes we first examine the portion of the runoff predictability due to land surface moisture that is attributable to knowledge of SWE. To do so, we subtract from the runoff variance explained by SOI, AO and SWE that explained by SOI and AO. In this way, runoff predictability due to SWE represents the incremental increase, above that due to climatic state, in explained runoff variance due to the knowledge of SWE alone. This is shown in Figure 9.

[34] As would be expected, SWE explains seasonal runoff variance most strongly where snow existing on the

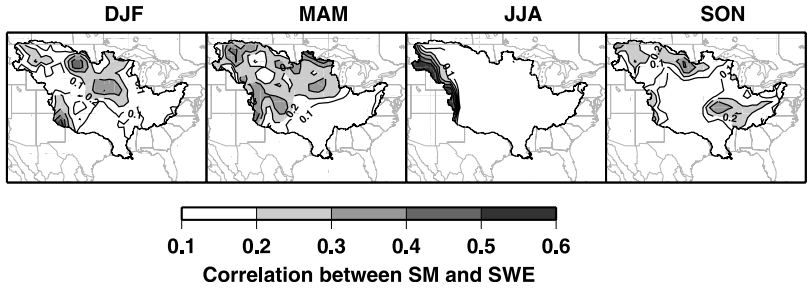

Figure 8. For each season, the correlation coefficient between the seasonal average SM and seasonal average SWE.

initialization date melts and forms runoff during the season being predicted. This can be seen most clearly at lead 0 in the northwestern portion of the basin. During DJF (at lead 0, using 30 November predictors) the correlations are strongest in the northwestern portion of the basin, while for MAM (28 February predictors) the area of high correlation retreats toward the mountains and the northern central area, and during JJA (31 May predictors) strong correlation is seen only in the Rocky Mountains on the western boundary of the basin. Referring to Figure 5, the predictability due to SWE coincides closely with the areas of highest runoff production, which illustrates the importance of snow, and its current operational use, in forecasting late spring and summer streamflow in the rivers originating in the western Mississippi River basin.

[35] At longer leads of two to three seasons, locally significant runoff predictability exists almost exclusively in isolated areas along the western boundary of the basin, which is again an anticipated result, as the snowpack disappears over virtually the entire basin each year, and deeper snowpacks that are capable of persisting longer than three seasons exist only in the highest mountains. JJA, which is the season with high runoff rates from the mountainous western areas of the basin, shows areas with locally significant runoff variance explained at a lead of two seasons, that is, JJA runoff is partially predictable from SWE information on 30 November. Although at the scale of the entire Mississippi basin this spatially limited response does not exhibit field significance, regional analyses could reveal useful predictability at a lead of two seasons. The current operational use of the snow state in spring-summer streamflow forecasts begins on 1 January; however, these results suggest that skillful forecasts could possibly begin at least one month earlier.

3.5. Runoff Predictability Due to Soil Moisture State

[36] The predictability due to SM was computed using the combined variance explained by the climatic and land surface predictors, and subtracting the variance explained by the combination of SOI, AO and SWE, and is shown in Figure 10. By estimating the predictability of runoff due to SM in this way, Figure 10 displays the increase in predictability due to SM knowledge beyond that already explained by climate signals and the SWE. Field significance in Figure 10 can be

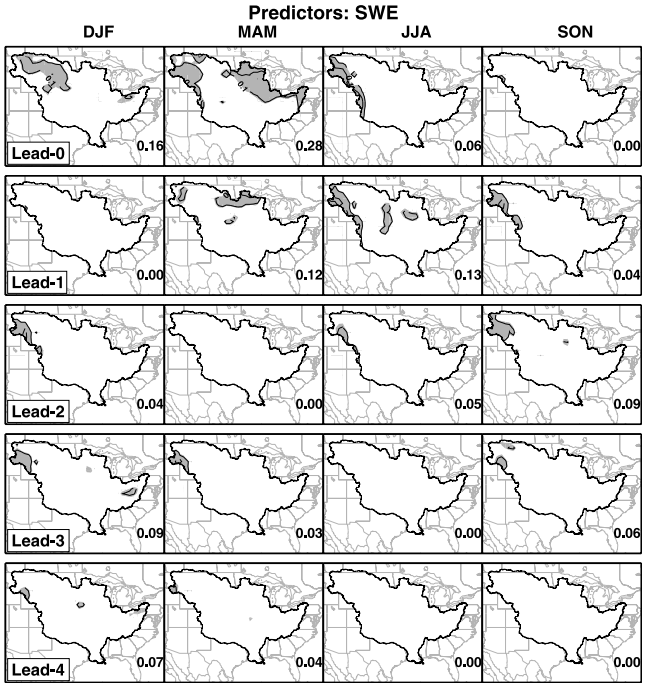

Figure 9. As for Figure 6, but showing the predictability due to SWE alone.

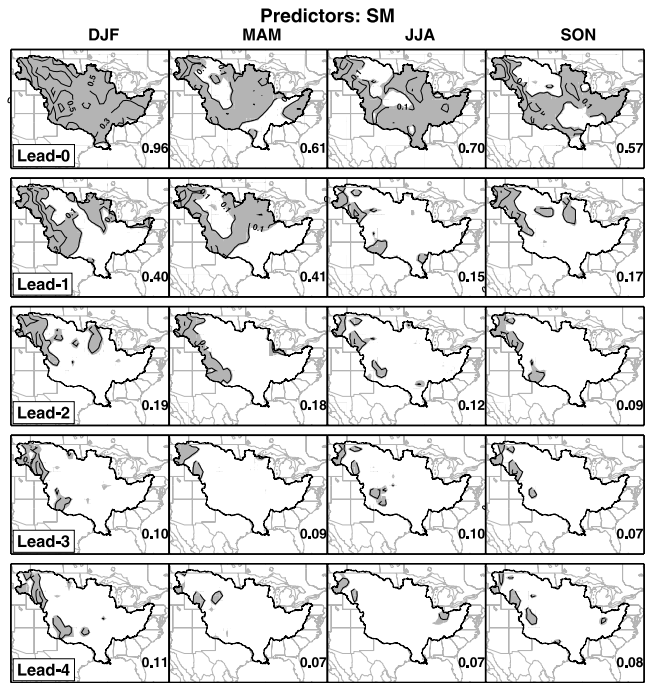

Figure 10. As for Figure 6, but showing the predictability of seasonal runoff due to SM alone.

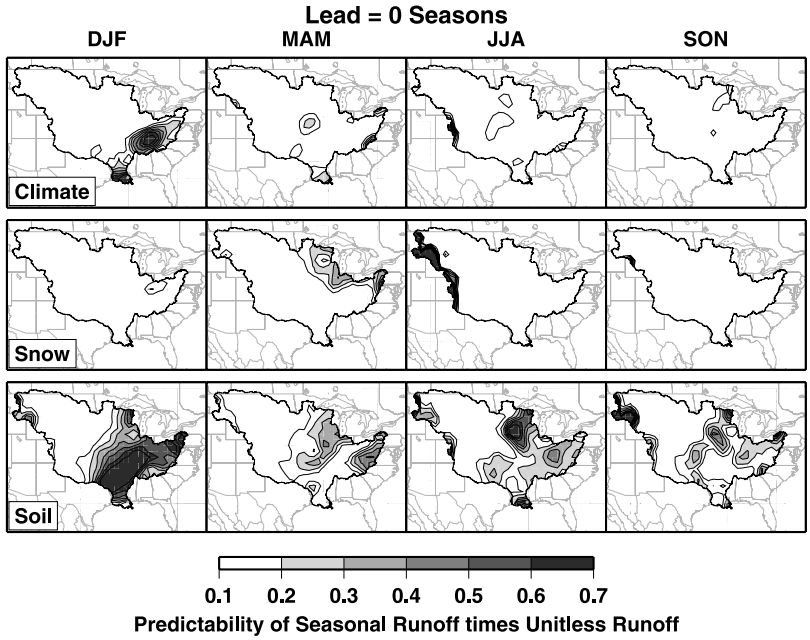

Figure 11. Unitless variable representing the importance of predictability. The variable is defined as the fraction of the runoff explained by the climate or land surface indicators (defined in the left panel for each row) times the unitless runoff (Figure 5), for a lead of 0 seasons.

claimed through a 4 season lead for DJF runoff prediction, and through 3 seasons for MAM and JJA runoff.

[37] The most prominent feature in Figure 10 is the larger area of the basin, as compared to climate predictors (Figure 7) or SWE (Figure 9) that shows statistically significant runoff variance explained for all seasons at lead 0. Although SM explains considerably greater DJF runoff variance than SWE at leads of one to two seasons for the western regions, this area produces relatively little runoff during this period so the value of the added predictability is lessened. During the intense JJA runoff from the mountainous west, SM provides a small but significant increase in explained runoff variance in pockets of the mountainous western boundary in addition to that achievable due to knowledge of snow state, indicating that despite the high correlation of SWE and SM in this area, significant independent information is obtained from each source. The areas showing the greatest JJA runoff (Figure 5), however, are still more highly correlated with SWE (Figure 9) than with SM (Figure 10).

[38] In general, for the western boundary of the Mississippi River basin, SM shows greater persistence than SWE, as indicated by higher levels of significant runoff variance

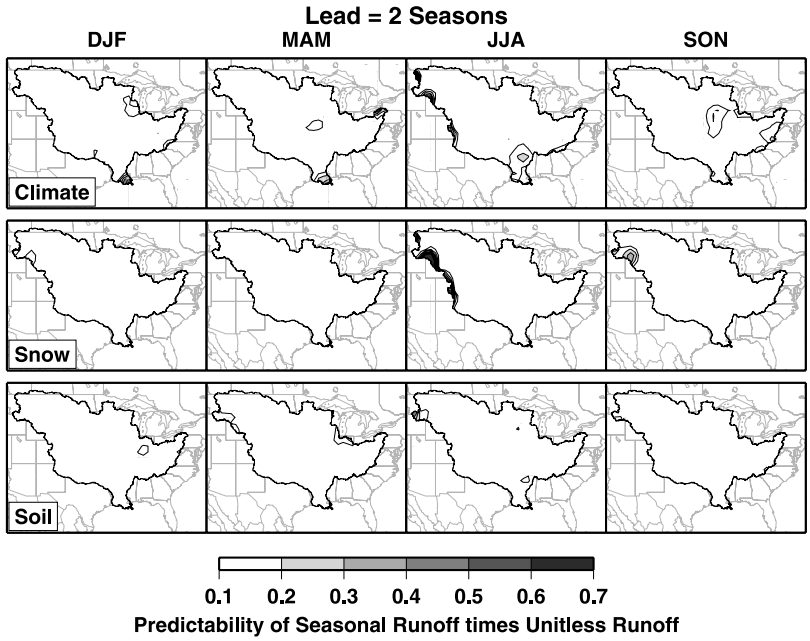

Figure 12. Same as for Figure 11, but for a lead of 2 seasons.

Table 2. Summary of Relative Importance of Predictors in Forecasting Seasonal Runoff[a]

	Lead (DJF)					Lead (MAM)					Lead (JJA)					Lead (SON)				
Predictors	0	1	2	3	4	0	1	2	3	4	0	1	2	3	4	0	1	2	3	4
SOI AO	158	**95**	**75**	**157**	**27**	90	83	**55**	**60**	**81**	90	93	**82**	**70**	**85**	58	**69**	**76**	**64**	**56**
SWE	21	0	6	23	23	94	26	0	4	19	120	**102**	47	4	5	3	21	30	18	1
SM	**441**	75	44	26	26	**189**	**89**	45	39	27	**278**	53	49	36	37	**228**	48	35	34	38

[a]Values are computed by multiplying at each grid cell the runoff variance explained by the predictors by the local unitless seasonal runoff, and summing these values over the Mississippi basin. Higher values indicate greater basin-wide predictability of seasonal runoff volume attributable to the predictor(s). Bold indicates the most influential factor for each season and lead.

explained at longer lead times. For example, SWE provides very little predictability of JJA runoff at a lead of three seasons, while significant SM influence is still seen. For an initialization date (date of forecast) of 31 August (i.e., lead-1 for DJF, lead-2 for MAM, lead-3 for JJA), snow is virtually absent from the basin, and can provide no forecast information, while SM shows significant explained runoff variance for DJF, MAM and JJA at leads through 3–4 seasons. This illustrates how knowledge of the SM and snow states can complement each other in a forecast setting, providing considerable independent information despite their correlation with each other.

3.6. Importance of Predictability Due to Defined Sources

[39] To quantify the importance of the climate indicators, SWE, and SM in forecasting runoff, a dimensionless variable is derived for each grid cell, and summed over the entire basin. The variable defined is the product of unitless runoff at each grid cell (Figure 5) and the variance explained by (1) SOI and AO (as in Figure 7); (2) SWE (Figure 9); and (3) SM (Figure 10) at each grid cell. Spatial plots of this variable are shown in Figures 11 and 12 for leads of 0 and 2 seasons, respectively. The basin-wide sum of this variable provides a snapshot of the relative importance of each source of predictive information in each season and at each lag. Table 2 presents these values for the entire Mississippi River basin. Most of our results (e.g., Figures 11 and 12) show distinct differences between the western and eastern portions of the basin Therefore Tables 3 and 4 provide the same variable, summed over areas west and east, respectively, of longitude 100°W.

[40] Figure 11 shows the dominance of SM for runoff prediction at a lead of 0 seasons throughout the basin, which is also supported by Table 2. It is also obvious from Figure 11 that knowledge of SWE in the mountainous western extreme of the basin provides the most important information for predicting JJA runoff, as discussed in section 3.4. It is interesting to note that the low levels of predictability of MAM runoff due to SWE at lead-0 in Figure 9 are absent from Figure 11, since the predictability affects a very small amount of runoff. Figure 11 also illustrates that despite low levels of predictability (approximately 10–20% of runoff variance explained) by soil moisture in the southeast for JJA runoff at a lead of 0 seasons, the high levels of runoff in this region accentuates the importance of predictability attributable to soil moisture.

[41] Table 2 indicates that the climate signal is dominant at leads of one season or more at the basin-wide scale for DJF and SON runoff, and at two seasons or more for MAM and JJA runoff. Examining the division of the basin in Tables 3 and 4, SWE provides the dominant source of JJA runoff predictability in the western portion of the basin through a lead of two seasons. SM provides the dominant influence on MAM runoff predictability in the west through a 2-season lead. The land surface signal, that is, SM and SWE combined, is a stronger predictor of runoff than the climate signal in the western portion of the basin, except for JJA runoff at lead-3 and lead-4, though again these cases have limited practical significance. For the eastern portion of the basin (Table 4) the climate signal is the dominant source of important runoff predictability at lead times of 1 season or more.

[42] Figure 12 shows that this dominance of the climate signal in runoff predictability at a lead of 2 seasons is very limited spatially, and is accompanied by no important predictability from the land surface. It is evident from Figure 12 that the values in Tables 2, 3, and 4 at leads of two seasons (or more, though no figure is shown) represent low predictability in spatially limited areas, with the SM and SWE generally only providing important predictability along the western edge of the basin, and climate information being focused in isolated pockets in the east and southeast. Long lead runoff predictability is geographically limited, and is largely due to modest levels of predictability (Figures 7, 9, and 10) in areas with high levels of runoff.

[43] The field significance of the dimensionless variables plotted in each panel of Figures 11 and 12 correspond to those for Figures 7, 9, and 10; that is, for Figure 11, scaled predictability due to climate and soil moisture are field significant in all seasons, while snow is not field significant for seasons JJA or SON. For Figure 12, the scaled predictability due to climate is field significant only for the DJF season, that due to snow is field significant only for SON, and soil moisture passes the field significance test for all seasons. Figures 11 and 12 show that if the interest is related to a sub-area of the Mississippi River basin, as would be typical for a water manager concerned with runoff contrib-

Table 3. Summary of Relative Importance of Predictors, as for Table 2, but Only for Regions West of Longitude 100°W

	Lead (DJF)					Lead (MAM)					Lead (JJA)					Lead (SON)				
Predictors	0	1	2	3	4	0	1	2	3	4	0	1	2	3	4	0	1	2	3	4
SOI AO	2	2	3	3	2	6	4	4	**5**	3	25	23	25	**28**	**25**	6	8	5	5	**6**
SWE	1	0	**6**	**4**	2	11	5	0	4	3	**120**	**78**	**39**	4	5	3	**21**	**15**	**9**	1
SM	**30**	**20**	4	3	3	**20**	**20**	**13**	4	**4**	44	18	16	11	10	**61**	12	8	7	5

Table 4. Summary of Relative Importance of Predictors, as for Table 2, but Only for Regions East of Longitude 100°W

	Lead (DJF)					Lead (MAM)					Lead (JJA)					Lead (SON)				
Predictors	0	1	2	3	4	0	1	2	3	4	0	1	2	3	4	0	1	2	3	4
SOI AO	156	**93**	**72**	**154**	**26**	84	**79**	**51**	**55**	**78**	65	**71**	**56**	**43**	**60**	52	**61**	**71**	**58**	**50**
SWE	20	0	0	19	21	84	21	0	0	16	0	23	8	0	0	0	0	14	9	0
SM	**411**	55	40	23	23	**169**	69	32	35	23	**234**	35	33	25	27	**168**	37	27	27	33

uting to a reservoir, for example, the basin-wide field significance is too stringent a test. Failure to pass the basin-wide field significance test applied in this study does not indicate that there is no important predictability in localized areas, however, a separate evaluation of the area of interest would be required.

4. Conclusions

[44] The predictability of runoff throughout the Mississippi River basin has been evaluated both spatially, and by season and prediction lead time. As surrogates for climate predictability, we used the SOI and the AO. In general, SOI used in a simple persistence mode (ignoring climatological knowledge of ENSO event evolution) was found to provide comparable information for our purposes to a statistical forecast of SOI.

[45] The climatic indicators provided a small but significant source of predictability for DJF runoff for leads of one through three seasons that exceeded that due to the land surface state, especially in the eastern portions of the Mississippi River basin. Because these climate indicators are readily available, this represents a source of predictability that can be exploited at present.

[46] In general, SM is the dominant source of runoff predictability at lead 0 in all seasons. When the basin was divided at longitude 100°W into western and eastern portions, SM provided the dominant source of predictability at lead-0 (which represents an average lead time of 1.5 months) in both regions, except in JJA in the western mountainous region, where SWE was most important. For lead times of 1.5 months, then, a better determination of soil moisture state can provide valuable predictive capability of runoff throughout the basin. For areas west of longitude 100°W, the land surface state generally has a stronger predictive capability than the climate indicators; whereas climate indicators are more important for eastern areas of the Mississippi basin at leads of one season or greater. Although SM and SWE are correlated to varying extents during certain seasons in different parts of the basin, they nonetheless can provide a level of significant independent information and complement each other for runoff predictability.

[47] Although modest (though statistically significant) DJF runoff predictability exists at a lead time of 3 seasons due to both climate and SM, much of this predictive capability is in areas producing little runoff, and is therefore of lessened practical importance. For JJA runoff in particular, locally significant runoff predictability, limited geographically to the western mountainous areas, at a lead of 2 seasons is coincident with high runoff producing areas. This information could be useful to water managers in the western Mississippi River basin, since it suggests the potential to provide skillful forecast information at lead times earlier than are currently used operationally, and there are large storage facilities allowing managers to respond to long lead forecasts.

[48] **Acknowledgments.** This publication was supported in part by the Joint Institute for the Study of the Atmosphere and Ocean (JISAO) at the University of Washington, funded under NOAA Cooperative Agreement NA17RJ1232, contribution 920, as part of the GEWEX Continental-Scale International Project (GCIP), and by a NASA Earth System Science Fellowship to the first author. This paper benefited from the careful reading of the manuscript and thoughtful comments of three anonymous reviewers. All statistical computations were performed using the GNU R software, freely available from www.r-project.org.

References

Baldwin, C. K., Seasonal streamflow forecasting using climate information, paper presented at 69th Western Snow Conference, West. Snow Conf., Sun Valley, Idaho, 16–19 April 2001.

Baldwin, M. P., and T. J. Dunkerton, Stratospheric harbingers of anomalous weather regimes, *Science*, *294*, 581–584, 2001.

Barnston, A. G., Linear statistical short-term climate predictive skill in the Northern Hemisphere, *J. Clim.*, *7*, 1513–1564, 1994.

Barnston, A. G., M. H. Glantz, and Y. He, Predictive skill of Statistical and dynamical climate models in SST forecasts during the 1997–98 El Niño episode and the 1998 La Niña onset, *Bull. Am. Meterol. Soc.*, *80*, 217–243, 1999.

Beard, D. P., Bureau of Reclamation revamps efforts to help fish, *Fisheries*, *19*, 6–7, 1994.

Beljaars, A. C. M., P. Viterbo, M. J. Miller, and A. K. Betts, The anomalous rainfall over the United States during July 1993: Sensitivity to land surface parameterization and soil moisture anomalies, *Mon. Weather Rev.*, *124*, 362–383, 1996.

Betts, A. K., J. H. Ball, A. C. M. Beljaars, M. J. Miller, and P. A. Viterbo, The land surface-atmospheric interaction: A review based on observational and global modeling perspectives, *J. Geophys. Res.*, *101*, 7209–7225, 1996.

Carroll, S. S., T. R. Carroll, and R. W. Poston, Spatial modeling and prediction of snow water equivalent using ground-based, airborne, and satellite snow data, *J. Geophys. Res.*, *104*, 19,623–19,629, 1999.

Cayan, D. R., K. T. Redmond, and L. G. Riddle, ENSO and hydrologic extremes in the western United States, *J. Clim.*, *12*, 2881–2893, 1999.

Cherkauer, K. A., L. C. Bowling, and D. P. Lettenmaier, Variable infiltration capacity (VIC) cold land process model updates, *Global Planet. Change*, in press, 2003.

Church, J. E., The human side of snow, *Sci. Mon.*, *44*, 137–149, 1937.

Dirmeyer, P. A., Problems in initializing soil wetness, *Bull. Am. Meteorol. Soc.*, *76*, 2234–2240, 1995.

Dracup, J. A., and E. Kahya, The relationships between U.S. streamflow and La Niña events, *Water Resour. Res.*, *30*, 2133–2141, 1994.

Fedorov, A. V., The response of the coupled tropical ocean-atmosphere to westerly wind bursts, *Q. J. R. Meteorol. Soc.*, *128*, 1–23, 2002.

Garen, D. C., Improved techniques in regression-based streamflow volume forecasting, *J. Water Resour. Plann. Manage.*, *118*, 654–670, 1992.

Garen, D. C., ENSO indicators and long-range climate forecasts: Usage in seasonal streamflow volume forecasting in the western United States, *Eos Trans. AGU*, *79*(45), Fall Meet. Suppl., F325, 1998.

Gershunov, A., ENSO influence on intraseasonal extreme rainfall and temperature frequencies in the contiguous United States: Implications for long-range predictability, *J. Clim.*, *11*, 3192–3203, 1998.

Goddard, L., S. J. Mason, S. E. Zebiak, C. F. Ropelewski, R. Basher, and M. A. Cane, Current approaches to seasonal-to-interannual climate predictions, *Int. J. Climatol.*, *12*, 1111–1152, 2001.

Goodison, B. E., and A. E. Walker, Canadian development and use of snow cover information from passive microwave satellite data, in *Passive Remote Sensing of Land-Atmosphere Interactions: ESA/NASA International Workshop, Utrecht, Netherlands*, edited by B. J. Choudhury et al., pp. 245–262, Eur. Space Agency, Paris, 1995.

Groisman, P. Y., and D. R. Legates, The accuracy of United States precipitation data, *Bull. Am. Meteorol. Soc.*, *75*, 215–227, 1994.

Hall, D. K., G. A. Riggs, V. V. Salomonson, N. DiGiromamo, and K. J. Bayr, MODIS snow cover products, *Remote Sens. Environ.*, *83*, 181–194, 2002.

Higgins, R. W., A. Leetmaa, Y. Xue, and A. Barnston, Dominant factors influencing the seasonal predictability of U.S. precipitation and surface air temperature, *J. Clim.*, *13*, 3994–4017, 2000.

Hornberger, G. M., et al., A plan for a new science initiative on the global water cycle, U.S. Global Change Res. Program, Washington, D. C., 2001.

Intergovernmental Panel on Climate Change, *Climate Change 2001: Impacts, Adaptation, and Vulnerability*, Cambridge Univ. Press, New York, 2001.

Kahya, E., and J. A. Dracup, U.S. streamflow patterns in relation to El Niño/Southern Oscillation, *Water Resour. Res.*, *29*, 2491–2503, 1993.

Kerr, Y. H., P. Waldteufel, J. P. Wigneron, J. Martinuzzi, J. Font, and M. Berger, Soil moisture retrieval from space: The Soil Moisture and Ocean Salinity (SMOS) mission, *IEEE Trans. Geosci. Remote Sens.*, *39*, 1729–1735, 2001.

Knaff, J. A., and C. W. Landsea, An El Niño-Southern Oscillation climatology and persistence (CLIPER) forecasting scheme, *Weather Forecast.*, *12*, 633–652, 1997.

Kumar, A., and M. P. Hoerling, Annual cycle of pacific-north American seasonal predictability associated with different phases of ENSO, *J. Clim.*, *11*, 3295–3308, 1998.

Kunkel, K. E., and J. R. Angel, Relationship of ENSO to snowfall and related cyclone activity in the contiguous United States, *J. Geophys. Res.*, *104*, 19,425–19,434, 1999.

Landsea, C. W., and J. A. Knaff, How much skill was there in forecasting the very strong 1997–98 El Niño?, *Bull. Am. Meteorol. Soc.*, *81*, 2107–2119, 2000.

Liang, X., D. P. Lettenmaier, E. Wood, and S. J. Burges, A simple hydrologically based model of land surface water and energy fluxes for general circulation models, *J. Geophys. Res.*, *99*, 14,415–14,428, 1994.

Lin, H., and J. Derome, A three-year lagged correlation between the North Atlantic Oscillation and winter conditions over the North Pacific and North America, *Geophys. Research Lett.*, *25*, 2829–2832, 1998.

Linsley, R. K., and W. C. Ackerman, Method of predicting the runoff from rainfall, *Trans. Am. Soc. Civ. Eng.*, *107*, 825–846, 1942.

Livezey, R. E., and W. Y. Chen, Statistical field significance and its determination by monte carlo techniques, *Mon. Weather Rev.*, *111*, 46–59, 1983.

Livezey, R. E., and T. M. Smith, Covariability of aspects of North American climate with global sea surface temperatures on interannual to interdecadal timescales, *J. Clim.*, *12*, 289–302, 1999.

Ma, X. L., Z. Wan, C. C. Moeller, W. P. Menzel, and L. E. Gumley, Simultaneous retrieval of atmospheric profiles, land-surface temperature, and surface emissivity from moderate-resolution imaging spectroradiometer thermal infrared data: Extension of a two-step algorithm, *Appl. Opt.*, *41*, 909–924, 2002.

Marston, E., The West's water-crats and dam-icans, in *Western Water Made Simple*, pp. 5–15, Island Press, Washington, D. C., 1987.

Maurer, E. P., A. W. Wood, J. C. Adam, D. P. Lettenmaier, and B. Nijssen, A long-term hydrologically-based data set of land surface fluxes and states for the conterminous United States, *J. Clim.*, *15*, 3237–3251, 2002.

McCabe, G. J., and M. D. Dettinger, Decadal variations in the strength of ENSO teleconnections with precipitation in the western U.S., *Int. J. Climatol.*, *19*, 1399–1410, 1999.

National Assessment Synthesis Team, *Climate Change Impacts on the United States: The Potential Consequences of Climate Variability and Change*, 620 pp., Cambridge Univ. Press, New York, 2001.

National Research Council, *Predictability and Limits-to-Prediction in Hydrologic Systems*, 118 pp., Natl. Acad. Press, Washington, D. C., 2002.

National Water and Climate Center, The NRCS water supply forecasting system, NWCC briefing paper, Natl. Resour. Conserv. Serv., U.S. Dep. of Agric., Washington, D. C., June 1998.

Njoku, E. G., and L. Li, Retrieval of land surface parameters using passive microwave measurements at 6–18 GHz, *IEEE Trans. Geosci. Remote Sens.*, *37*, 79–93, 1999.

Oglesby, R. J., S. Marshall, D. J. Erikson, J. O. Roads, and F. R. Robertson, Thresholds in atmosphere-soil moisture interactions: Results from climate model studies, *J. Geophys. Res.*, *107*(D14), 4224, doi:10.1029/2001JD001045, 2002.

Pauwels, V. R. N., R. Hoeben, N. E. C. Verhoest, and F. P. De Troch, The importance of spatial patterns of remotely sensed soil moisture in the improvement of discharge predictions for small-scale basins through data assimilation, *J. Hydrol. Amsterdam*, *251*, 88–102, 2001.

Philander, S. G., El Niño and La Niña predictable climate fluctuations, *Rep. Prog. Phys.*, *62*, 123–142, 1999.

Plummer, J. L., Western water resources: The desert is blooming, but will it continue?, *Water Resour. Bull.*, *30*, 595–603, 1994.

Potts, H. L., Snow-surveys and runoff-forecasting from photographs, *Eos. Trans. AGU*, *18*, 658–660, 1937.

Rango, A., and J. Martinec, Application of a snowmelt-runoff model using Landsat data, *Nord. Hydrol.*, *10*, 225–238, 1979.

Rango, A., A. E. Walker, and B. E. Goodison, Snow and ice, in *Remote Sensing in Hydrology and Water Management*, edited by G. A. Schultz and E. T. Engman, pp. 239–262, Springer-Verlag, New York, 2000.

Rasmussen, E. M., and J. M. Wallace, Meteorological aspects of the El Niño/Southern Oscillation, *Science*, *222*, 1195–1202, 1983.

Rohli, R. V., A. J. Vega, M. R. Binkley, S. D. Britton, H. E. Heckman, J. M. Jenkins, Y. Ono, and D. E. Sheeler, Surface and 700 hPa atmospheric circulation patterns for the Great Lakes basin and eastern North America and relationship to atmospheric telecommunications, *J. Great Lakes Res.*, *25*, 45–60, 1999.

Ropelewski, C. F., and P. D. Jones, An extension of the Tahiti-Darwin Southern Oscillation Index, *Mon. Weather Rev.*, *115*, 2161–2165, 1987.

Schaake, J. C., et al., Another statistical look at LDAS soil moisture fields, paper presented at 16th Conference on Hydrology, Am. Meteorol. Soc., Orlando, Fla., 13–17 Jan. 2002.

Shi, J., and J. Dozier, Estimation of snow water equivalence using SIR-C/X-SAR. I. Inferring snow density and subsurface properties, *IEEE Trans. Geosci. Remote Sens.*, *38*, 2465–2473, 2000.

Shukla, J., Predictability in the midst of chaos: A scientific basis for climate forecasting, *Science*, *282*, 728–731, 1998.

Soil Conservation Service, Snow surveys and water supply forecasting, *Agric. Inf. Bull. U. S. Dep. Agric.*, *536*, 1988.

Thompson, D. W. J., and J. M. Wallace, The Arctic Oscillation signature in the wintertime geopotential height and temperature fields, *Geophys. Res. Lett.*, *25*, 1297–1300, 1998.

Thompson, D. W. J., and J. M. Wallace, Annular modes in the extratropical circulation, Part I: Month-to-month variability, *J. Clim.*, *13*, 1000–1016, 2000.

Trenberth, K. E., The definition of El Niño, *Bull. Am. Meteorol. Soc.*, *78*, 2771–2777, 1997.

Twedt, T. M., J. C. Schaake, and E. L. Peck, National Weather Service extended streamflow prediction, paper presented at 45th Annual Meeting of the Western Snow Conference, West. Snow Conf., Albuquerque, N. M., 18–21 April 1977.

U.S. Census Bureau, Annual projections of the total resident population as of July 1: 1999–2100, *Natl. Population Projection Summary File NP-T1*, Populations Projection Program, Washington, D. C., 2000.

Vörösmarty, C. J., P. Green, J. Salisbury, and R. B. Lammers, Global water resources: vulnerability from climate change and population growth, *Science*, *289*, 284–288, 2000.

Walker, J. P., and P. R. Houser, A methodology for initializing soil moisture in a global climate model: Assimilation of near surface soil moisture observations, *J. Geophys. Res.*, *106*, 11,761–11,774, 2001.

Wang, H., M. Ting, and M. Ji, Prediction of seasonal mean United States precipitation based on El Niño seas surface temperatures, *Geophys. Res. Lett.*, *26*, 1341–1344, 1999.

Western Water Policy Review Advisory Commission, *Water in the West: The Challenge for the Next Century*, Arlington, Va., 1998.

Wolter, K., R. M. Dole, and C. A. Smith, Short-term climate extremes over the continental United States and ENSO. Part I: Seasonal temperatures, *J. Clim.*, *12*, 3255–3272, 1999.

Wood, A. W., E. P. Maurer, A. Kumar, and D. P. Lettenmaier, Long-range experimental hydrologic forecasting for the eastern United States, *J. Geophys. Res.*, *107*(D20), 4429, doi:10.1029/2001JD000659, 2002.

World Meteorological Organization, Scientific plan for the GEWEX Continental-Scale International Project (GCIP), *WCRP-67 WMO/TD 61,*65 pp., Geneva, 1992.

D. P. Lettenmaier and E. P. Maurer, Department of Civil and Environmental Engineering, University of Washington, Box 352700, Seattle, WA 98195, USA. (dennisl@u.washington.edu; edm@atmos.washington.edu)